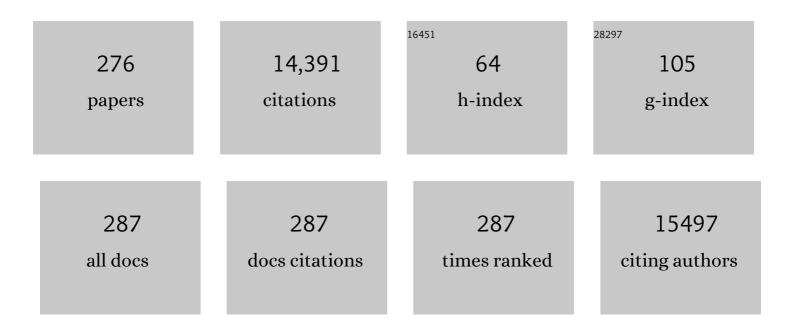
Victor S Batista

List of Publications by Year in descending order

Source: https://exaly.com/author-pdf/3957525/publications.pdf Version: 2024-02-01



| # | Article | IF | CITATIONS |
|----|---|------|-----------|
| 1 | Nitrogen-doped tungsten carbide nanoarray as an efficient bifunctional electrocatalyst for water splitting in acid. Nature Communications, 2018, 9, 924. | 12.8 | 571 |
| 2 | Active sites of copper-complex catalytic materials for electrochemical carbon dioxide reduction. Nature Communications, 2018, 9, 415. | 12.8 | 527 |
| 3 | Electrochemical CO ₂ Reduction to Hydrocarbons on a Heterogeneous Molecular Cu Catalyst in Aqueous Solution. Journal of the American Chemical Society, 2016, 138, 8076-8079. | 13.7 | 450 |
| 4 | Quantum Dynamics Simulations of Interfacial Electron Transfer in Sensitized TiO2Semiconductors. Journal of the American Chemical Society, 2003, 125, 7989-7997. | 13.7 | 368 |
| 5 | Quantum Mechanics/Molecular Mechanics Study of the Catalytic Cycle of Water Splitting in Photosystem II. Journal of the American Chemical Society, 2008, 130, 3428-3442. | 13.7 | 345 |
| 6 | Light-driven water oxidation for solar fuels. Coordination Chemistry Reviews, 2012, 256, 2503-2520. | 18.8 | 337 |
| 7 | Intramolecular Proton Transfer Boosts Water Oxidation Catalyzed by a Ru Complex. Journal of the American Chemical Society, 2015, 137, 10786-10795. | 13.7 | 246 |
| 8 | Robust resistive memory devices using solution-processable metal-coordinated azoÂaromatics. Nature Materials, 2017, 16, 1216-1224. | 27.5 | 244 |
| 9 | Facet-Dependent Photoelectrochemical Performance of TiO ₂ Nanostructures: An Experimental and Computational Study. Journal of the American Chemical Society, 2015, 137, 1520-1529. | 13.7 | 242 |
| 10 | Stable iridium dinuclear heterogeneous catalysts supported on metal-oxide substrate for solar water oxidation. Proceedings of the National Academy of Sciences of the United States of America, 2018, 115, 2902-2907. | 7.1 | 229 |
| 11 | S ₁ -State Model of the O ₂ -Evolving Complex of Photosystem II. Biochemistry, 2011, 50, 6308-6311. | 2.5 | 210 |
| 12 | Investigating the Role of Copper Oxide in Electrochemical CO ₂ Reduction in Real Time. ACS Applied Materials & Interfaces, 2018, 10, 8574-8584. | 8.0 | 207 |
| 13 | Influence of Thermal Fluctuations on Interfacial Electron Transfer in Functionalized TiO2 Semiconductors. Journal of the American Chemical Society, 2005, 127, 18234-18242. | 13.7 | 196 |
| 14 | Allosteric pathways in imidazole glycerol phosphate synthase. Proceedings of the National Academy of Sciences of the United States of America, 2012, 109, E1428-36. | 7.1 | 192 |
| 15 | Multihole water oxidation catalysis on haematite photoanodes revealed by operando spectroelectrochemistry and DFT. Nature Chemistry, 2020, 12, 82-89. | 13.6 | 189 |
| 16 | The O ₂ -Evolving Complex of Photosystem II: Recent Insights from Quantum Mechanics/Molecular Mechanics (QM/MM), Extended X-ray Absorption Fine Structure (EXAFS), and Femtosecond X-ray Crystallography Data. Accounts of Chemical Research, 2017, 50, 41-48. | 15.6 | 168 |
| 17 | Acetylacetonate Anchors for Robust Functionalization of TiO ₂ Nanoparticles with Mn(II)â^'Terpyridine Complexes. Journal of the American Chemical Society, 2008, 130, 14329-14338. | 13.7 | 151 |
| 18 | Functional Role of Pyridinium during Aqueous Electrochemical Reduction of CO ₂ on Pt(111). Journal of Physical Chemistry Letters, 2013, 4, 745-748. | 4.6 | 146 |

| # | Article | IF | CITATIONS |
|----|---|------|-----------|
| 19 | Reduction of Systematic Uncertainty in DFT Redox Potentials of Transition-Metal Complexes. Journal of Physical Chemistry C, 2012, 116, 6349-6356. | 3.1 | 145 |
| 20 | Eigenvector centrality for characterization of protein allosteric pathways. Proceedings of the National Academy of Sciences of the United States of America, 2018, 115, E12201-E12208. | 7.1 | 145 |
| 21 | Search for Catalysts by Inverse Design: Artificial Intelligence, Mountain Climbers, and Alchemists. Chemical Reviews, 2019, 119, 6595-6612. | 47.7 | 142 |
| 22 | Semiclassical molecular dynamics simulations of excited state double-proton transfer in 7-azaindole dimers. Journal of Chemical Physics, 1999, 110, 9922-9936. | 3.0 | 138 |
| 23 | QM/MM Models of the O2-Evolving Complex of Photosystem II. Journal of Chemical Theory and Computation, 2006, 2, 1119-1134. | 5.3 | 136 |
| 24 | Structural–Functional Role of Chloride in Photosystem II. Biochemistry, 2011, 50, 6312-6315. | 2.5 | 132 |
| 25 | Electric field stimulates production of highly conductive microbial OmcZ nanowires. Nature Chemical Biology, 2020, 16, 1136-1142. | 8.0 | 112 |
| 26 | A Model of the Oxygen-Evolving Center of Photosystem II Predicted by Structural Refinement Based on EXAFS Simulations. Journal of the American Chemical Society, 2008, 130, 6728-6730. | 13.7 | 110 |
| 27 | Electronic π-Delocalization Boosts Catalytic Water Oxidation by Cu(II) Molecular Catalysts Heterogenized on Graphene Sheets. Journal of the American Chemical Society, 2017, 139, 12907-12910. | 13.7 | 108 |
| 28 | Covalent Attachment of a Rhenium Bipyridyl CO ₂ Reduction Catalyst to Rutile TiO ₂ . Journal of the American Chemical Society, 2011, 133, 6922-6925. | 13.7 | 106 |
| 29 | Protospacer Adjacent Motif-Induced Allostery Activates CRISPR-Cas9. Journal of the American Chemical Society, 2017, 139, 16028-16031. | 13.7 | 104 |
| 30 | CO ₂ Reduction Catalysts on Gold Electrode Surfaces Influenced by Large Electric Fields. Journal of the American Chemical Society, 2018, 140, 17643-17655. | 13.7 | 103 |
| 31 | Hydroxamate Anchors for Improved Photoconversion in Dye-Sensitized Solar Cells. Inorganic Chemistry, 2013, 52, 6752-6764. | 4.0 | 102 |
| 32 | Characterization of synthetic oxomanganese complexes and the inorganic core of the O2-evolving complex in photosystem II: Evaluation of the DFT/B3LYP level of theory. Journal of Inorganic Biochemistry, 2006, 100, 786-800. | 3.5 | 99 |
| 33 | Water-stable, hydroxamate anchors for functionalization of TiO2 surfaces with ultrafast interfacial electron transfer. Energy and Environmental Science, 2010, 3, 917. | 30.8 | 99 |
| 34 | QM/MM Study of Energy Storage and Molecular Rearrangements Due to the Primary Event in Vision. Biophysical Journal, 2004, 87, 2931-2941. | 0.5 | 98 |
| 35 | S ₀ -State Model of the Oxygen-Evolving Complex of Photosystem II. Biochemistry, 2013, 52, 7703-7706. | 2.5 | 97 |
| 36 | Hydroxamate anchors for water-stable attachment to TiO2 nanoparticles. Energy and Environmental Science, 2009, 2, 1173. | 30.8 | 91 |

| # | Article | IF | CITATIONS |
|----|--|---------------|-----------|
| 37 | Ultrathin dendrimer–graphene oxide composite film for stable cycling lithium–sulfur batteries. Proceedings of the National Academy of Sciences of the United States of America, 2017, 114, 3578-3583. | 7.1 | 90 |
| 38 | Phenothiazine Radical Cation Excited States as Super-oxidants for Energy-Demanding Reactions. Journal of the American Chemical Society, 2018, 140, 5290-5299. | 13.7 | 89 |
| 39 | A tridentate Ni pincer for aqueous electrocatalytic hydrogen production. New Journal of Chemistry, 2012, 36, 1149. | 2.8 | 88 |
| 40 | Mechanistic Insights into Surface Chemical Interactions between Lithium Polysulfides and Transition Metal Oxides. Journal of Physical Chemistry C, 2017, 121, 14222-14227. | 3.1 | 86 |
| 41 | Role of Tensorial Electronic Friction in Energy Transfer at Metal Surfaces. Physical Review Letters, 2016, 116, 217601. | 7.8 | 85 |
| 42 | Femtosecond photoelectron spectroscopy of the I2â^ anion: A semiclassical molecular dynamics simulation method. Journal of Chemical Physics, 1999, 110, 3736-3747. | 3.0 | 84 |
| 43 | Tensor-Train Split-Operator Fourier Transform (TT-SOFT) Method: Multidimensional Nonadiabatic Quantum Dynamics. Journal of Chemical Theory and Computation, 2017, 13, 4034-4042. | 5.3 | 84 |
| 44 | Ultrafast Photooxidation of Mn(II)â^'Terpyridine Complexes Covalently Attached to TiO ₂ Nanoparticles. Journal of Physical Chemistry C, 2007, 111, 11982-11990. | 3.1 | 82 |
| 45 | A Selfâ€Improved Waterâ€Oxidation Catalyst: Is One Site Really Enough?. Angewandte Chemie - International Edition, 2014, 53, 205-209. | 13.8 | 82 |
| 46 | Deposition of an oxomanganese water oxidation catalyst on TiO2 nanoparticles: computational modeling, assembly and characterization. Energy and Environmental Science, 2009, 2, 230. | 30.8 | 80 |
| 47 | Inverse Design and Synthesis of acac-Coumarin Anchors for Robust TiO ₂ Sensitization. Journal of the American Chemical Society, 2011, 133, 9014-9022. | 13.7 | 79 |
| 48 | Heterogenized Iridium Water-Oxidation Catalyst from a Silatrane Precursor. ACS Catalysis, 2016, 6, 5371-5377. | 11.2 | 79 |
| 49 | Key role of the REC lobe during CRISPR–Cas9 activation by â€~sensing', â€~regulating', and â€~lockingâ catalytic HNH domain. Quarterly Reviews of Biophysics, 2018, 51, . | €™ the 5.7 | 79 |
| 50 | Behavior of the Ru-bda Water Oxidation Catalyst Covalently Anchored on Glassy Carbon Electrodes. ACS Catalysis, 2015, 5, 3422-3429. | 11.2 | 78 |
| 51 | Allosteric Motions of the CRISPR–Cas9 HNH Nuclease Probed by NMR and Molecular Dynamics. Journal of the American Chemical Society, 2020, 142, 1348-1358. | 13.7 | 78 |
| 52 | Matching-pursuit for simulations of quantum processes. Journal of Chemical Physics, 2003, 118, 6720-6724. | 3.0 | 77 |
| 53 | Interfacial Structure and Electric Field Probed by <i>in Situ</i> Electrochemical Vibrational Stark Effect Spectroscopy and Computational Modeling. Journal of Physical Chemistry C, 2017, 121, 18674-18682. | 3.1 | 77 |
| 54 | Implausibility of the vibrational theory of olfaction. Proceedings of the National Academy of Sciences of the United States of America, 2015, 112, E2766-74. | 7.1 | 76 |

| # | Article | IF | CITATIONS |
|----|---|------|-----------|
| 55 | Computational Studies of the Primary Phototransduction Event in Visual Rhodopsin. Accounts of Chemical Research, 2006, 39, 184-193. | 15.6 | 75 |
| 56 | Chiral Sum Frequency Generation for In Situ Probing Proton Exchange in Antiparallel β-Sheets at Interfaces. Journal of the American Chemical Society, 2013, 135, 3592-3598. | 13.7 | 74 |
| 57 | <i>Ab initio</i> tensorial electronic friction for molecules on metal surfaces: Nonadiabatic vibrational relaxation. Physical Review B, 2016, 94, . | 3.2 | 74 |
| 58 | Analysis of the Radiation-Damage-Free X-ray Structure of Photosystem II in Light of EXAFS and QM/MM Data. Biochemistry, 2015, 54, 1713-1716. | 2.5 | 73 |
| 59 | Efficient Multiphoton Sampling of Molecular Vibronic Spectra on a Superconducting Bosonic Processor. Physical Review X, 2020, 10, . | 8.9 | 73 |
| 60 | Amphiphilic Adsorption of Human Islet Amyloid Polypeptide Aggregates to Lipid/Aqueous Interfaces. Journal of Molecular Biology, 2012, 421, 537-547. | 4.2 | 71 |
| 61 | QM/MM computational studies of substrate water binding to the oxygen-evolving centre of photosystem II. Philosophical Transactions of the Royal Society B: Biological Sciences, 2008, 363, 1149-1156. | 4.0 | 70 |
| 62 | Bioinspired High-Potential Porphyrin Photoanodes. Journal of Physical Chemistry C, 2012, 116, 4892-4902. | 3.1 | 69 |
| 63 | End-On Bound Iridium Dinuclear Heterogeneous Catalysts on WO ₃ for Solar Water Oxidation. ACS Central Science, 2018, 4, 1166-1172. | 11.3 | 69 |
| 64 | NH ₃ Binding to the S ₂ State of the O ₂ -Evolving Complex of Photosystem II: Analogue to H ₂ O Binding during the S ₂ → S ₃ Transition. Biochemistry, 2015, 54, 5783-5786. | 2.5 | 68 |
| 65 | Semiclassical molecular dynamics simulations of ultrafast photodissociation dynamics associated with the Chappuis band of ozone. Journal of Chemical Physics, 1998, 108, 498-510. | 3.0 | 65 |
| 66 | Nonadiabatic photodissociation dynamics of ICN in the $\tilde{A}f$ continuum: A semiclassical initial value representation study. Journal of Chemical Physics, 2000, 112, 5566-5575. | 3.0 | 65 |
| 67 | Solution Structures of Highly Active Molecular Ir Water-Oxidation Catalysts from Density Functional Theory Combined with High-Energy X-ray Scattering and EXAFS Spectroscopy. Journal of the American Chemical Society, 2016, 138, 5511-5514. | 13.7 | 63 |
| 68 | Computational insights into the O2-evolving complex of photosystem II. Photosynthesis Research, 2008, 97, 91-114. | 2.9 | 62 |
| 69 | S ₃ State of the O ₂ -Evolving Complex of Photosystem II: Insights from QM/MM, EXAFS, and Femtosecond X-ray Diffraction. Biochemistry, 2016, 55, 981-984. | 2.5 | 62 |
| 70 | Matching-pursuit/split-operator-Fourier-transform simulations of excited-state nonadiabatic quantum dynamics in pyrazine. Journal of Chemical Physics, 2006, 125, 124313. | 3.0 | 61 |
| 71 | Characterization of Proton Coupled Electron Transfer in a Biomimetic Oxomanganese Complex: Evaluation of the DFT B3LYP Level of Theory. Journal of Chemical Theory and Computation, 2010, 6, 755-760. | 5.3 | 61 |
| 72 | Smelling Sulfur: Copper and Silver Regulate the Response of Human Odorant Receptor OR2T11 to Low-Molecular-Weight Thiols. Journal of the American Chemical Society, 2016, 138, 13281-13288. | 13.7 | 60 |

| # | Article | IF | CITATIONS |
|----|---|-------------------------------|---------------------|
| 73 | Semiclassical molecular dynamics simulations of intramolecular proton transfer in photoexcited 2-(2′-hydroxyphenyl)–oxazole. Journal of Chemical Physics, 2000, 113, 9510-9522. | 3.0 | 59 |
| 74 | Hydrophobic CuO Nanosheets Functionalized with Organic Adsorbates. Journal of the American Chemical Society, 2018, 140, 1824-1833. | 13.7 | 59 |
| 75 | <i>In Situ</i> Identification of Reaction Intermediates and Mechanistic Understandings of Methane Oxidation over Hematite: A Combined Experimental and Theoretical Study. Journal of the American Chemical Society, 2020, 142, 17119-17130. | 13.7 | 59 |
| 76 | Crystallographic Data Support the Carousel Mechanism of Water Supply to the Oxygen-Evolving Complex of Photosystem II. ACS Energy Letters, 2017, 2, 2299-2306. | 17.4 | 58 |
| 77 | High-resolution cryo-electron microscopy structure of photosystem II from the mesophilic cyanobacterium, <i>Synechocystis</i> sp. PCC 6803. Proceedings of the National Academy of Sciences of the United States of America, 2022, 119, . | 7.1 | 58 |
| 78 | Photoinduced electron transfer from rylenediimide radical anions and dianions to Re(bpy)(CO) ₃ using red and near-infrared light. Chemical Science, 2017, 8, 3821-3831. | 7.4 | 57 |
| 79 | Molecular mechanism of activation of human musk receptors OR5AN1 and OR1A1 by (<i>R</i>) Tj ETQq1 1 0.78 Sciences of the United States of America, 2018, 115, E3950-E3958. | 34314 rgB ⁻ 7.1 | 「 /Overlock] 57 |
| 80 | Efficiency of Interfacial Electron Transfer from Zn-Porphyrin Dyes into TiO ₂ Correlated to the Linker Single Molecule Conductance. Journal of Physical Chemistry C, 2013, 117, 24462-24470. | 3.1 | 55 |
| 81 | Altering the allosteric pathway in IGPS suppresses millisecond motions and catalytic activity. Proceedings of the National Academy of Sciences of the United States of America, 2017, 114, E3414-E3423. | 7.1 | 55 |
| 82 | Activation of OR1A1 suppresses PPAR-γ expression by inducing HES-1 in cultured hepatocytes. International Journal of Biochemistry and Cell Biology, 2015, 64, 75-80. | 2.8 | 54 |
| 83 | Real time path integrals using the Herman–Kluk propagator. Journal of Chemical Physics, 2002, 116, 2748-2756. | 3.0 | 53 |
| 84 | Heterogenized Molecular Catalysts: Vibrational Sum-Frequency Spectroscopic, Electrochemical, and Theoretical Investigations. Accounts of Chemical Research, 2019, 52, 1289-1300. | 15.6 | 53 |
| 85 | Ultrafast Photoinduced Interfacial Proton Coupled Electron Transfer from CdSe Quantum Dots to 4,4′-Bipyridine. Journal of the American Chemical Society, 2016, 138, 884-892. | 13.7 | 52 |
| 86 | Coherent Control in the Presence of Intrinsic Decoherence: Proton Transfer in Large Molecular Systems. Physical Review Letters, 2002, 89, 143201. | 7.8 | 51 |
| 87 | Stable Iridium(IV) Complexes of an Oxidation-Resistant Pyridine-Alkoxide Ligand: Highly Divergent Redox Properties Depending on the Isomeric Form Adopted. Journal of the American Chemical Society, 2015, 137, 7243-7250. | 13.7 | 51 |
| 88 | Antimony Complexes for Electrocatalysis: Activity of a Mainâ€Group Element in Proton Reduction. Angewandte Chemie - International Edition, 2017, 56, 9111-9115. | 13.8 | 51 |
| 89 | Quantum tunneling dynamics in multidimensional systems: A matching-pursuit description. Journal of Chemical Physics, 2004, 121, 1676-1680. | 3.0 | 50 |
| 90 | Crucial Role of Nuclear Dynamics for Electron Injection in a Dye–Semiconductor Complex. Journal of Physical Chemistry Letters, 2015, 6, 2393-2398. | 4.6 | 49 |

| # | Article | IF | CITATIONS |
|-----|--|------|-----------|
| 91 | Accurate Line Shapes from Sub-1 cm ^{–1} Resolution Sum Frequency Generation Vibrational Spectroscopy of α-Pinene at Room Temperature. Journal of Physical Chemistry A, 2015, 119, 1292-1302. | 2.5 | 49 |
| 92 | Photoexcited radical anion super-reductants for solar fuels catalysis. Coordination Chemistry Reviews, 2018, 361, 98-119. | 18.8 | 49 |
| 93 | Orientation of a Series of CO2 Reduction Catalysts on Single Crystal TiO2 Probed by Phase-Sensitive Vibrational Sum Frequency Generation Spectroscopy (PS-VSFG). Journal of Physical Chemistry C, 2012, 116, 24107-24114. | 3.1 | 48 |
| 94 | Electrochemical Reduction of CO ₂ Catalyzed by Re(pyridine-oxazoline)(CO) ₃ Cl Complexes. Inorganic Chemistry, 2017, 56, 3214-3226. | 4.0 | 48 |
| 95 | A Self-Consistent Space-Domain Decomposition Method for QM/MM Computations of Protein Electrostatic Potentials. Journal of Chemical Theory and Computation, 2006, 2, 175-186. | 5.3 | 47 |
| 96 | Interfacial electron transfer in photoanodes based on phosphorus(v) porphyrin sensitizers co-deposited on SnO2 with the Ir(III)Cp* water oxidation precatalyst. Journal of Materials Chemistry A, 2015, 3, 3868-3879. | 10.3 | 47 |
| 97 | Structural Changes in the Oxygen-Evolving Complex of PhotosystemÂll Induced by the S ₁ to S ₂ Transition: A Combined XRD and QM/MM Study. Biochemistry, 2014, 53, 6860-6862. | 2.5 | 46 |
| 98 | Ferroceneâ€Promoted Longâ€Cycle Lithium–Sulfur Batteries. Angewandte Chemie - International Edition, 2016, 55, 14818-14822. | 13.8 | 46 |
| 99 | Orientation of Cyano-Substituted Bipyridine Re(I) <i>fac</i> -Tricarbonyl Electrocatalysts Bound to Conducting Au Surfaces. Journal of Physical Chemistry C, 2016, 120, 1657-1665. | 3.1 | 46 |
| 100 | Facet-Dependent Kinetics and Energetics of Hematite for Solar Water Oxidation Reactions. ACS Applied Materials & M | 8.0 | 46 |
| 101 | QM/MM Study of the NMR Spectroscopy of the Retinyl Chromophore in Visual Rhodopsin. Journal of Chemical Theory and Computation, 2005, 1, 674-685. | 5.3 | 45 |
| 102 | Intrinsic electronic conductivity of individual atomically resolved amyloid crystals reveals micrometer-long hole hopping via tyrosines. Proceedings of the National Academy of Sciences of the United States of America, 2021, 118, . | 7.1 | 45 |
| 103 | Surface-Induced Anisotropic Binding of a Rhenium CO ₂ -Reduction Catalyst on Rutile TiO ₂ (110) Surfaces. Journal of Physical Chemistry C, 2016, 120, 20970-20977. | 3.1 | 44 |
| 104 | Nanotechnology for catalysis and solar energy conversion. Nanotechnology, 2021, 32, 042003. | 2.6 | 44 |
| 105 | Model study of coherent quantum dynamics of hole states in functionalized semiconductor nanostructures. Journal of Chemical Physics, 2005, 122, 154709. | 3.0 | 43 |
| 106 | Electrode-Ligand Interactions Dramatically Enhance CO ₂ Conversion to CO by the [Ni(cyclam)](PF ₆) ₂ Catalyst. ACS Catalysis, 2017, 7, 5282-5288. | 11.2 | 43 |
| 107 | Experimental and Theoretical Study of CO ₂ Insertion into Ruthenium Hydride Complexes. Inorganic Chemistry, 2016, 55, 1623-1632. | 4.0 | 42 |
| 108 | Observation of a potential-dependent switch of water-oxidation mechanism on Co-oxide-based catalysts. CheM, 2021, 7, 2101-2117. | 11.7 | 42 |

| # | Article | IF | CITATIONS |
|-----|--|------|-----------|
| 109 | Mechanism of Manganese-Catalyzed Oxygen Evolution from Experimental and Theoretical Analyses of ¹⁸ 0 Kinetic Isotope Effects. ACS Catalysis, 2015, 5, 7104-7113. | 11.2 | 41 |
| 110 | Electron Transfer Assisted by Vibronic Coupling from Multiple Modes. Journal of Chemical Theory and Computation, 2017, 13, 6000-6009. | 5.3 | 41 |
| 111 | Allosteric Pathways in the PPAR $\hat{1}^3$ -RXR $\hat{1}\pm$ nuclear receptor complex. Scientific Reports, 2016, 6, 19940. | 3.3 | 39 |
| 112 | Fundamental Role of Oxygen Stoichiometry in Controlling the Band Gap and Reactivity of Cupric Oxide Nanosheets. Journal of the American Chemical Society, 2016, 138, 10978-10985. | 13.7 | 39 |
| 113 | Dissecting Dynamic Allosteric Pathways Using Chemically Related Small-Molecule Activators. Structure, 2016, 24, 1155-1166. | 3.3 | 38 |
| 114 | Energetics of the S ₂ State Spin Isomers of the Oxygen-Evolving Complex of Photosystem II. Journal of Physical Chemistry B, 2017, 121, 1020-1025. | 2.6 | 38 |
| 115 | Visible Light Sensitization of TiO ₂ Surfaces with Alq3 Complexes. Journal of Physical Chemistry C, 2010, 114, 1317-1325. | 3.1 | 37 |
| 116 | Water-Nucleophilic Attack Mechanism for the Cu ^{II} (pyalk) ₂ Water-Oxidation Catalyst. ACS Catalysis, 2018, 8, 7952-7960. | 11.2 | 37 |
| 117 | Electrostatic Effects on Proton Coupled Electron Transfer in Oxomanganese Complexes Inspired by the Oxygen-Evolving Complex of Photosystem II. Journal of Physical Chemistry B, 2013, 117, 6217-6226. | 2.6 | 36 |
| 118 | Single Molecule Rectification Induced by the Asymmetry of a Single Frontier Orbital. Journal of Chemical Theory and Computation, 2014, 10, 3393-3400. | 5.3 | 36 |
| 119 | Hard templating ultrathin polycrystalline hematite nanosheets: effect of nano-dimension on CO ₂ to CO conversion via the reverse water-gas shift reaction. Nanoscale, 2017, 9, 12984-12995. | 5.6 | 36 |
| 120 | Strongly Coupled Phenazine–Porphyrin Dyads: Light-Harvesting Molecular Assemblies with Broad Absorption Coverage. ACS Applied Materials & Interfaces, 2019, 11, 8000-8008. | 8.0 | 36 |
| 121 | Coherent Control of Quantum Dynamics with Sequences of Unitary Phase-Kick Pulses. Annual Review of Physical Chemistry, 2009, 60, 293-320. | 10.8 | 35 |
| 122 | Fuel selection for a regenerative organic fuel cell/flow battery: thermodynamic considerations. Energy and Environmental Science, 2012, 5, 9534. | 30.8 | 35 |
| 123 | NMR and computational methods for molecular resolution of allosteric pathways in enzyme complexes. Biophysical Reviews, 2020, 12, 155-174. | 3.2 | 35 |
| 124 | Decrypting the Information Exchange Pathways across the Spliceosome Machinery. Journal of the American Chemical Society, 2020, 142, 8403-8411. | 13.7 | 35 |
| 125 | Computational Design of Intrinsic Molecular Rectifiers Based on Asymmetric Functionalization of <i>N</i> -Phenylbenzamide. Journal of Chemical Theory and Computation, 2015, 11, 5888-5896. | 5.3 | 34 |
| 126 | Controlling the rectification properties of molecular junctions through molecule–electrode coupling. Nanoscale, 2016, 8, 16357-16362. | 5.6 | 33 |

| # | Article | IF | CITATIONS |
|-----|--|------|-----------|
| 127 | Allosteric Communication Disrupted by a Small Molecule Binding to the Imidazole Glycerol Phosphate Synthase Protein–Protein Interface. Biochemistry, 2016, 55, 6484-6494. | 2.5 | 33 |
| 128 | The role of metals in mammalian olfaction of low molecular weight organosulfur compounds. Natural Product Reports, 2017, 34, 529-557. | 10.3 | 33 |
| 129 | Decelerating Charge Recombination Using Fluorinated Porphyrins in <i>N,N</i> -Bis(3,4,5-trimethoxyphenyl)aniline—Aluminum(III) Porphyrin—Fullerene Reaction Center Models. Journal of the American Chemical Society, 2020, 142, 10008-10024. | 13.7 | 33 |
| 130 | Model Study of Coherent-Control of the Femtosecond Primary Event of Vision. Journal of Physical Chemistry B, 2004, 108, 6745-6749. | 2.6 | 32 |
| 131 | QM/MM Model of the Mouse Olfactory Receptor MOR244-3 Validated by Site-Directed Mutagenesis Experiments. Biophysical Journal, 2014, 107, L5-L8. | 0.5 | 32 |
| 132 | A full set of iridium(<scp>iv</scp>) pyridine-alkoxide stereoisomers: highly geometry-dependent redox properties. Chemical Science, 2017, 8, 1642-1652. | 7.4 | 32 |
| 133 | Nanosecond Dynamics Regulate the MIFâ€Induced Activity of CD74. Angewandte Chemie - International Edition, 2018, 57, 7116-7119. | 13.8 | 32 |
| 134 | Computational Insights on Crystal Structures of the Oxygen-Evolving Complex of Photosystem II with Either Ca ²⁺ or Ca ²⁺ Substituted by Sr ²⁺ . Biochemistry, 2015, 54, 820-825. | 2.5 | 31 |
| 135 | Direct Interfacial Electron Transfer from High-Potential Porphyrins into Semiconductor Surfaces: A Comparison of Linkers and Anchoring Groups. Journal of Physical Chemistry C, 2018, 122, 13529-13539. | 3.1 | 31 |
| 136 | Catalytic manganese oxide nanostructures for the reverse water gas shift reaction. Nanoscale, 2019, 11, 16677-16688. | 5.6 | 31 |
| 137 | Characterization of Parallel β-Sheets at Interfaces by Chiral Sum Frequency Generation Spectroscopy. Journal of Physical Chemistry Letters, 2015, 6, 1310-1315. | 4.6 | 30 |
| 138 | Molecular titanium–hydroxamate complexes as models for TiO ₂ surface binding. Chemical Communications, 2016, 52, 2972-2975. | 4.1 | 30 |
| 139 | The structural basis for cancer drug interactions with the catalytic and allosteric sites of SAMHD1. Proceedings of the National Academy of Sciences of the United States of America, 2018, 115, E10022-E10031. | 7.1 | 30 |
| 140 | Proton exit pathways surrounding the oxygen evolving complex of photosystem II. Biochimica Et Biophysica Acta - Bioenergetics, 2021, 1862, 148446. | 1.0 | 30 |
| 141 | Protein nanowires with tunable functionality and programmable self-assembly using sequence-controlled synthesis. Nature Communications, 2022, 13, 829. | 12.8 | 30 |
| 142 | Ultrafast Vibrational Frequency Shifts Induced by Electronic Excitations: Naphthols in Low Dielectric Media. Journal of Physical Chemistry A, 2012, 116, 2775-2790. | 2.5 | 29 |
| 143 | Sum Frequency Generation Spectroscopy and Molecular Dynamics Simulations Reveal a Rotationally Fluid Adsorption State of α-Pinene on Silica. Journal of Physical Chemistry C, 2016, 120, 12578-12589. | 3.1 | 29 |
| 144 | Exploring Allosteric Pathways of a V-Type Enzyme with Dynamical Perturbation Networks. Journal of Physical Chemistry B, 2019, 123, 3452-3461. | 2.6 | 29 |

| # | Article | IF | CITATIONS |
|-----|--|------|-----------|
| 145 | Copper-mediated thiol potentiation and mutagenesis-guided modeling suggest a highly conserved copper-binding motif in human OR2M3. Cellular and Molecular Life Sciences, 2020, 77, 2157-2179. | 5.4 | 29 |
| 146 | High-Potential Porphyrins Supported on SnO ₂ and TiO ₂ Surfaces for Photoelectrochemical Applications. Journal of Physical Chemistry C, 2016, 120, 28971-28982. | 3.1 | 28 |
| 147 | Unusual Stability of a Bacteriochlorin Electrocatalyst under Reductive Conditions. A Case Study on CO ₂ Conversion to CO. ACS Catalysis, 2018, 8, 10131-10136. | 11.2 | 28 |
| 148 | A 300-fold conductivity increase in microbial cytochrome nanowires due to temperature-induced restructuring of hydrogen bonding networks. Science Advances, 2022, 8, eabm7193. | 10.3 | 28 |
| 149 | Unusual kinetics of thermal decay of dim-light photoreceptors in vertebrate vision. Proceedings of the National Academy of Sciences of the United States of America, 2014, 111, 10438-10443. | 7.1 | 27 |
| 150 | Can TDDFT Describe Excited Electronic States of Naphthol Photoacids? A Closer Look with EOM-CCSD. Journal of Chemical Theory and Computation, 2018, 14, 867-876. | 5.3 | 27 |
| 151 | Behavior of Ru–bda Waterâ€Oxidation Catalysts in Low Oxidation States. Chemistry - A European Journal, 2018, 24, 12838-12847. | 3.3 | 27 |
| 152 | Enhanced specificity mutations perturb allosteric signaling in CRISPR-Cas9. ELife, 2021, 10, . | 6.0 | 27 |
| 153 | Theoretical EXAFS studies of a model of the oxygenâ€evolving complex of photosystem II obtained with the quantum cluster approach. International Journal of Quantum Chemistry, 2013, 113, 474-478. | 2.0 | 26 |
| 154 | Correlating Photoacidity to Hydrogen-Bond Structure by Using the Local O–H Stretching Probe in Hydrogen-Bonded Complexes of Aromatic Alcohols. Journal of Physical Chemistry A, 2015, 119, 4800-4812. | 2.5 | 26 |
| 155 | Quantitative structure-property relationship model leading to virtual screening of fullerene derivatives: Exploring structural attributes critical for photoconversion efficiency of polymer solar cell acceptors. Nano Energy, 2016, 26, 677-691. | 16.0 | 25 |
| 156 | Vibrational Stark shift spectroscopy of catalysts under the influence of electric fields at electricde–solution interfaces. Chemical Science, 2021, 12, 10131-10149. | 7.4 | 25 |
| 157 | Ultrafast Solventâ€Assisted Electronic Level Crossing in 1â€Naphthol. Angewandte Chemie - International Edition, 2013, 52, 6871-6875. | 13.8 | 24 |
| 158 | Formate to Oxalate: A Crucial Step for the Conversion of Carbon Dioxide into Multi arbon Compounds. ChemCatChem, 2016, 8, 3453-3457. | 3.7 | 24 |
| 159 | Triplet–triplet energy transfer in artificial and natural photosynthetic antennas. Proceedings of the National Academy of Sciences of the United States of America, 2017, 114, E5513-E5521. | 7.1 | 24 |
| 160 | High-Energy Charge-Separated States by Reductive Electron Transfer Followed by Electron Shift in the Tetraphenylethylene–Aluminum(III) Porphyrin–Fullerene Triad. Journal of Physical Chemistry C, 2019, 123, 131-143. | 3.1 | 24 |
| 161 | Fabrication of Modularly Functionalizable Microcapsules Using Protein-Based Technologies. ACS Biomaterials Science and Engineering, 2016, 2, 1856-1861. | 5.2 | 23 |
| 162 | Electron–Hole-Pair-Induced Vibrational Energy Relaxation of Rhenium Catalysts on Gold Surfaces. Journal of Physical Chemistry Letters, 2018, 9, 406-412. | 4.6 | 22 |

| # | Article | IF | CITATIONS |
|-----|---|------|-----------|
| 163 | Molecular design of light-harvesting photosensitizers: effect of varied linker conjugation on interfacial electron transfer. Physical Chemistry Chemical Physics, 2016, 18, 18678-18682. | 2.8 | 21 |
| 164 | Thermodynamics of the S ₂ -to-S ₃ state transition of the oxygen-evolving complex of photosystem II. Physical Chemistry Chemical Physics, 2019, 21, 20840-20848. | 2.8 | 21 |
| 165 | Is Deprotonation of the Oxygen-Evolving Complex of Photosystem II during the S ₁ → S ₂ Transition Suppressed by Proton Quantum Delocalization?. Journal of the American Chemical Society, 2021, 143, 8324-8332. | 13.7 | 21 |
| 166 | Linker Rectifiers for Covalent Attachment of Transitionâ€Metal Catalysts to Metalâ€Oxide Surfaces. ChemPhysChem, 2014, 15, 1138-1147. | 2.1 | 20 |
| 167 | Time-Sliced Thawed Gaussian Propagation Method for Simulations of Quantum Dynamics. Journal of Physical Chemistry A, 2016, 120, 3260-3269. | 2.5 | 20 |
| 168 | Thousandfold Enhancement of Photoreduction Lifetime in Re(bpy)(CO) ₃ via Spin-Dependent Electron Transfer from a Perylenediimide Radical Anion Donor. Journal of the American Chemical Society, 2017, 139, 16466-16469. | 13.7 | 20 |
| 169 | Charge Transport and Rectification in Donor–Acceptor Dyads. Journal of Physical Chemistry C, 2017, 121, 19053-19062. | 3.1 | 20 |
| 170 | Chiral Inversion of Amino Acids in Antiparallel β-Sheets at Interfaces Probed by Vibrational Sum Frequency Generation Spectroscopy. Journal of Physical Chemistry B, 2019, 123, 5769-5781. | 2.6 | 20 |
| 171 | Regulation of MIF Enzymatic Activity by an Allosteric Site at the Central Solvent Channel. Cell Chemical Biology, 2020, 27, 740-750.e5. | 5.2 | 20 |
| 172 | Reply to Turin et al.: Vibrational theory of olfaction is implausible. Proceedings of the National Academy of Sciences of the United States of America, 2015, 112, E3155. | 7.1 | 19 |
| 173 | Beyond Local Group Modes in Vibrational Sum Frequency Generation. Journal of Physical Chemistry A, 2015, 119, 3407-3414. | 2.5 | 18 |
| 174 | Characterization of Protein Tyrosine Phosphatase 1B Inhibition by Chlorogenic Acid and Cichoric Acid. Biochemistry, 2017, 56, 96-106. | 2.5 | 18 |
| 175 | D1-S169A Substitution of Photosystem II Perturbs Water Oxidation. Biochemistry, 2019, 58, 1379-1387. | 2.5 | 18 |
| 176 | Relative stability of the S2 isomers of the oxygen evolving complex of photosystem II. Photosynthesis Research, 2019, 141, 331-341. | 2.9 | 18 |
| 177 | The Effect of (â^')-Epigallocatechin-3-Gallate on the Amyloid-β Secondary Structure. Biophysical Journal, 2020, 119, 349-359. | 0.5 | 18 |
| 178 | New Insights from Sum Frequency Generation Vibrational Spectroscopy into the Interactions of Islet Amyloid Polypeptides with Lipid Membranes. Journal of Diabetes Research, 2016, 2016, 1-17. | 2.3 | 17 |
| 179 | Assessment of DFT for Computing Sum Frequency Generation Spectra of an Epoxydiol and a Deuterated Isotopologue at Fused Silica/Vapor Interfaces. Journal of Physical Chemistry B, 2016, 120, 1919-1927. | 2.6 | 17 |
| 180 | Collaboration between experiment and theory in solar fuels research. Chemical Society Reviews, 2019, 48, 1865-1873. | 38.1 | 17 |

| # | Article | IF | CITATIONS |
|-----|---|------|-----------|
| 181 | The MP/SOFT methodology for simulations of quantum dynamics: Model study of the photoisomerization of the retinyl chromophore in visual rhodopsin. Journal of Photochemistry and Photobiology A: Chemistry, 2007, 190, 274-282. | 3.9 | 16 |
| 182 | MoD-QM/MM Structural Refinement Method: Characterization of Hydrogen Bonding in the <i>Oxytricha nova</i> G-Quadruplex. Journal of Chemical Theory and Computation, 2014, 10, 5125-5135. | 5.3 | 16 |
| 183 | Insights into Photosystem II from Isomorphous Difference Fourier Maps of Femtosecond X-ray Diffraction Data and Quantum Mechanics/Molecular Mechanics Structural Models. ACS Energy Letters, 2017, 2, 397-407. | 17.4 | 16 |
| 184 | Inclusion of nuclear quantum effects for simulations of nonlinear spectroscopy. Journal of Chemical Physics, 2018, 148, 244105. | 3.0 | 16 |
| 185 | A conductive metal–organic framework photoanode. Chemical Science, 2020, 11, 9593-9603. | 7.4 | 16 |
| 186 | The O–H Stretching Mode of a Prototypical Photoacid as a Local Dielectric Probe. Journal of Physical Chemistry A, 2011, 115, 10511-10516. | 2.5 | 15 |
| 187 | Triplet Oxygen Evolution Catalyzed by a Biomimetic Oxomanganese Complex: Functional Role of the Carboxylate Buffer. ACS Catalysis, 2015, 5, 2384-2390. | 11.2 | 15 |
| 188 | Vibronic Effects in the Ultrafast Interfacial Electron Transfer of Perylene-Sensitized TiO ₂ Surfaces. Journal of Physical Chemistry C, 2019, 123, 12599-12607. | 3.1 | 15 |
| 189 | Water Network Dynamics Next to the Oxygen-Evolving Complex of Photosystem II. Inorganics, 2019, 7, 39. | 2.7 | 15 |
| 190 | Community Network Analysis of Allosteric Proteins. Methods in Molecular Biology, 2021, 2253, 137-151. | 0.9 | 15 |
| 191 | Electrochemical Reduction of Aqueous Imidazolium on Pt(111) by Proton Coupled Electron Transfer. Topics in Catalysis, 2015, 58, 23-29. | 2.8 | 14 |
| 192 | Preparation of Halogenated Fluorescent Diaminophenazine Building Blocks. Journal of Organic Chemistry, 2015, 80, 9881-9888. | 3.2 | 14 |
| 193 | Hot Hole Hopping in a Polyoxotitanate Cluster Terminated with Catechol Electron Donors. Journal of Physical Chemistry C, 2016, 120, 20006-20015. | 3.1 | 14 |
| 194 | Ammonia Binding in the Second Coordination Sphere of the Oxygen-Evolving Complex of Photosystem II. Biochemistry, 2016, 55, 4432-4436. | 2.5 | 14 |
| 195 | Unanticipated Stickiness of α-Pinene. Journal of Physical Chemistry A, 2017, 121, 3239-3246. | 2.5 | 14 |
| 196 | X-ray Free Electron Laser Radiation Damage through the S-State Cycle of the Oxygen-Evolving Complex of Photosystem II. Journal of Physical Chemistry B, 2017, 121, 9382-9388. | 2.6 | 14 |
| 197 | Multi-time formulation of Matsubara dynamics. Journal of Chemical Physics, 2019, 151, 034108. | 3.0 | 14 |
| 198 | Linker Length-Dependent Electron-Injection Dynamics of Trimesitylporphyrins on SnO ₂ Films. Journal of Physical Chemistry C, 2017, 121, 22690-22699. | 3.1 | 13 |

| # | Article | IF | CITATIONS |
|-----|---|-----|-----------|
| 199 | Inverse Design of a Catalyst for Aqueous CO/CO ₂ Conversion Informed by the Ni ^{II} –Iminothiolate Complex. Inorganic Chemistry, 2018, 57, 15474-15480. | 4.0 | 13 |
| 200 | Hammett neural networks: prediction of frontier orbital energies of tungsten–benzylidyne photoredox complexes. Chemical Science, 2019, 10, 6844-6854. | 7.4 | 13 |
| 201 | High-Conductance Conformers in Histograms of Single-Molecule Current–Voltage Characteristics. Journal of Physical Chemistry C, 2014, 118, 8316-8321. | 3.1 | 12 |
| 202 | Interfacial Electron Transfer Followed by Photooxidation in <i>N</i> , <i>N</i> -Bis(<i>p</i> -anisole)aminopyridine–Aluminum(III) Porphyrin–Titanium(IV) Oxide Self-Assembled Photoanodes. Journal of Physical Chemistry C, 2017, 121, 14484-14497. | 3.1 | 12 |
| 203 | Antimony Complexes for Electrocatalysis: Activity of a Mainâ€Group Element in Proton Reduction. Angewandte Chemie, 2017, 129, 9239-9243. | 2.0 | 12 |
| 204 | Characterization of ammonia binding to the second coordination shell of the oxygen-evolving complex of photosystem II. Dalton Transactions, 2017, 46, 16089-16095. | 3.3 | 12 |
| 205 | Mechanism of Inhibition of the Reproduction of SARS-CoV-2 and <i>Ebola</i> Viruses by Remdesivir. Biochemistry, 2021, 60, 1869-1875. | 2.5 | 12 |
| 206 | Structural Basis for Reduced Dynamics of Three Engineered HNH Endonuclease Lys-to-Ala Mutants for the Clustered Regularly Interspaced Short Palindromic Repeat (CRISPR)-Associated 9 (CRISPR/Cas9) Enzyme. Biochemistry, 2022, 61, 785-794. | 2.5 | 12 |
| 207 | Ferroceneâ€Promoted Long ycle Lithium–Sulfur Batteries. Angewandte Chemie, 2016, 128, 15038-15042. | 2.0 | 11 |
| 208 | Ring-polymer, centroid, and mean-field approximations to multi-time Matsubara dynamics. Journal of Chemical Physics, 2020, 153, 124112. | 3.0 | 11 |
| 209 | Do crystallographic XFEL data support binding of a water molecule to the oxygen-evolving complex of photosystem II exposed to two flashes of light?. Proceedings of the National Academy of Sciences of the United States of America, 2021, 118, . | 7.1 | 11 |
| 210 | Quantum Dynamics of the Excited‣tate Intramolecular Proton Transfer in 2â€(2′â€Hydroxyphenyl)benzothiazole. Israel Journal of Chemistry, 2009, 49, 187-197. | 2.3 | 10 |
| 211 | Floquet Study of Quantum Control of the Cis–Trans Photoisomerization of Rhodopsin. Journal of Chemical Theory and Computation, 2018, 14, 1198-1205. | 5.3 | 10 |
| 212 | Carbon chain shape selectivity by the mouse olfactory receptor OR-17. Organic and Biomolecular Chemistry, 2018, 16, 2541-2548. | 2.8 | 10 |
| 213 | Dopant-Dependent SFG Response of Rhenium CO ₂ Reduction Catalysts Chemisorbed on SrTiO ₃ (100) Single Crystals. Journal of Physical Chemistry C, 2018, 122, 13944-13952. | 3.1 | 10 |
| 214 | Regioselective Ultrafast Photoinduced Electron Transfer from Naphthols to Halocarbon Solvents. Journal of Physical Chemistry Letters, 2019, 10, 2657-2662. | 4.6 | 10 |
| 215 | Effect of Electronic Coupling on Electron Transfer Rates from Photoexcited Naphthalenediimide Radical Anion to Re(bpy)(CO) ₃ X. Journal of Physical Chemistry C, 2019, 123, 10178-10190. | 3.1 | 10 |
| 216 | Atmospheric β-Caryophyllene-Derived Ozonolysis Products at Interfaces. ACS Earth and Space Chemistry, 2019, 3, 158-169. | 2.7 | 10 |

| # | Article | IF | CITATIONS |
|-----|--|------|-----------|
| 217 | Surprisingly big linker-dependence of activity and selectivity in CO ₂ reduction by an iridium(<scp>i</scp>) pincer complex. Chemical Communications, 2020, 56, 9126-9129. | 4.1 | 10 |
| 218 | Computational insights into the membrane fusion mechanism of SARS-CoV-2 at the cellular level. Computational and Structural Biotechnology Journal, 2021, 19, 5019-5028. | 4.1 | 10 |
| 219 | Insights into Binding of Single-Stranded Viral RNA Template to the Replication–Transcription Complex of SARS-CoV-2 for the Priming Reaction from Molecular Dynamics Simulations. Biochemistry, 2022, 61, 424-432. | 2.5 | 10 |
| 220 | Functional Tensor-Train Chebyshev Method for Multidimensional Quantum Dynamics Simulations. Journal of Chemical Theory and Computation, 2022, 18, 25-36. | 5.3 | 10 |
| 221 | Two-dimensional Raman spectroscopy of Lennard-Jones liquids via ring-polymer molecular dynamics. Journal of Chemical Physics, 2020, 153, 034117. | 3.0 | 9 |
| 222 | Tensor-Train Split-Operator KSL (TT-SOKSL) Method for Quantum Dynamics Simulations. Journal of Chemical Theory and Computation, 2022, 18, 3327-3346. | 5.3 | 9 |
| 223 | Orientations of nonlocal vibrational modes from combined experimental and theoretical sum frequency spectroscopy. Chemical Physics Letters, 2017, 683, 199-204. | 2.6 | 8 |
| 224 | Ultrafast photo-induced charge transfer of 1-naphthol and 2-naphthol to halocarbon solvents. Chemical Physics Letters, 2017, 683, 49-56. | 2.6 | 8 |
| 225 | Distinct Binding of Rhenium Catalysts on Nanostructured and Single-Crystalline TiO ₂ Surfaces Revealed by Two-Dimensional Sum Frequency Generation Spectroscopy. Journal of Physical Chemistry C, 2018, 122, 26018-26031. | 3.1 | 8 |
| 226 | Iterative Power Algorithm for Global Optimization with Quantics Tensor Trains. Journal of Chemical Theory and Computation, 2021, 17, 3280-3291. | 5.3 | 8 |
| 227 | Heterogeneous Composition of Oxygen-Evolving Complexes in Crystal Structures of Dark-Adapted Photosystem II. Biochemistry, 2021, 60, 3374-3384. | 2.5 | 8 |
| 228 | Distinct allosteric pathways in imidazole glycerol phosphate synthase from yeast and bacteria. Biophysical Journal, 2022, 121, 119-130. | 0.5 | 8 |
| 229 | Semiclassical Molecular Dynamics Simulations of the Excited State Photodissociation Dynamics of H2O in the A1B1Bandâ€. Journal of Physical Chemistry B, 2002, 106, 8271-8277. | 2.6 | 7 |
| 230 | Structure–function relationships in single molecule rectification by N-phenylbenzamide derivatives. New Journal of Chemistry, 2016, 40, 7373-7378. | 2.8 | 7 |
| 231 | Effects of aligned αâ€helix peptide dipoles on experimental electrostatic potentials. Protein Science, 2017, 26, 1692-1697. | 7.6 | 7 |
| 232 | On the relationship between cumulative correlation coefficients and the quality of crystallographic data sets. Protein Science, 2017, 26, 2410-2416. | 7.6 | 7 |
| 233 | Thermodynamic and Structural Factors That Influence the Redox Potentials of Tungsten–Alkylidyne Complexes. ACS Catalysis, 2017, 7, 6134-6143. | 11.2 | 7 |
| 234 | A Multispecific Investigation of the Metal Effect in Mammalian Odorant Receptors for Sulfur-Containing Compounds. Chemical Senses, 2018, 43, 357-366. | 2.0 | 7 |

| # | Article | IF | CITATIONS |
|-----|--|------|-----------|
| 235 | Robust Binding of Disulfide-Substituted Rhenium Bipyridyl Complexes for CO2 Reduction on Gold Electrodes. Frontiers in Chemistry, 2020, 8, 86. | 3.6 | 7 |
| 236 | A structurally preserved allosteric site in the MIF superfamily affects enzymatic activity and CD74 activation in D-dopachrome tautomerase. Journal of Biological Chemistry, 2021, 297, 101061. | 3.4 | 7 |
| 237 | MptpA Kinetics Enhanced by Allosteric Control of an Active Conformation. Journal of Molecular Biology, 2022, 434, 167540. | 4.2 | 7 |
| 238 | Probing the remarkable thermal kinetics of visual rhodopsin with E181Q and S186A mutants. Journal of Chemical Physics, 2017, 146, 215104. | 3.0 | 6 |
| 239 | Semiconductor-to-conductor transition in 2D copper(<scp>ii</scp>) oxide nanosheets through surface sulfur-functionalization. Nanoscale, 2020, 12, 14549-14559. | 5.6 | 6 |
| 240 | Development of an Enantioselective Synthesis of (â^')-Euonyminol. Journal of Organic Chemistry, 2021, 86, 17011-17035. | 3.2 | 6 |
| 241 | Energy Flow Under Control. Science, 2009, 326, 245-246. | 12.6 | 5 |
| 242 | Ultraviolet vision: photophysical properties of the unprotonated retinyl Schiff base in the Siberian hamster cone pigment. Theoretical Chemistry Accounts, 2016, 135, 1. | 1.4 | 5 |
| 243 | Inferring Protonation States of Hydroxamate Adsorbates on TiO ₂ Surfaces. Journal of Physical Chemistry C, 2017, 121, 11985-11990. | 3.1 | 5 |
| 244 | Ultrafast proton-assisted tunneling through ZrO ₂ in dye-sensitized SnO ₂ -core/ZrO ₂ -shell films. Chemical Communications, 2018, 54, 7971-7974. | 4.1 | 5 |
| 245 | Vibronic Dynamics of Photodissociating ICN from Simulations of Ultrafast Xâ€Ray Absorption Spectroscopy. Angewandte Chemie - International Edition, 2020, 59, 20044-20048. | 13.8 | 5 |
| 246 | Identification of a Na ⁺ -Binding Site near the Oxygen-Evolving Complex of Spinach Photosystem II. Biochemistry, 2020, 59, 2823-2831. | 2.5 | 5 |
| 247 | Allosteric Impact of the Variable Insert Loop in <i>Vaccinia</i> H1-Related (VHR) Phosphatase. Biochemistry, 2020, 59, 1896-1908. | 2.5 | 5 |
| 248 | Organometallic Iridium Complex Containing a Dianionic, Tridentate, Mixed Organic–Inorganic Ligand. Inorganic Chemistry, 2016, 55, 8121-8129. | 4.0 | 4 |
| 249 | Classical Optimal Control for Energy Minimization Based On Diffeomorphic Modulation under Observable-Response-Preserving Homotopy. Journal of Chemical Theory and Computation, 2018, 14, 3351-3362. | 5.3 | 4 |
| 250 | D1-S169A substitution of photosystem II reveals a novel S2-state structure. Biochimica Et Biophysica Acta - Bioenergetics, 2020, 1861, 148301. | 1.0 | 4 |
| 251 | Selective Heterogeneous Transfer Hydrogenation from Tertiary Amines to Alkynes. ACS Catalysis, 2021, 11, 5405-5415. | 11.2 | 4 |
| 252 | Tuning the Conduction Band for Interfacial Electron Transfer: Dye-Sensitized Sn _{<i>x</i>} Ti _{1–<i>x</i>} O ₂ Photoanodes for Water Splitting. ACS Applied Energy Materials, 2021, 4, 4695-4703. | 5.1 | 4 |

| # | Article | IF | CITATIONS |
|-----|---|-----|-----------|
| 253 | Chapter 1. Inverse molecular design for materials discovery. Chemical Modelling, 2013, , 1-31. | 0.4 | 4 |
| 254 | Binding of the substrate analog methanol in the oxygen-evolving complex of photosystem II in the D1-N87A genetic variant of cyanobacteria. Faraday Discussions, 2022, 234, 195-213. | 3.2 | 4 |
| 255 | Multiple unitary-pulses for coherent-control of tunnelling and decoherence. Journal of Modern Optics, 2007, 54, 2617-2627. | 1.3 | 3 |
| 256 | Tunneling through Coulombic barriers: quantum control of nuclear fusion. Molecular Physics, 2012, 110, 995-999. | 1.7 | 3 |
| 257 | Kepler Predictor–Corrector Algorithm: Scattering Dynamics with One-Over-R Singular Potentials. Journal of Chemical Theory and Computation, 2012, 8, 24-35. | 5.3 | 3 |
| 258 | Steered Quantum Dynamics for Energy Minimization. Journal of Physical Chemistry B, 2015, 119, 715-727. | 2.6 | 3 |
| 259 | Facile solvolysis of a surprisingly twisted tertiary amide. New Journal of Chemistry, 2016, 40, 1974-1981. | 2.8 | 3 |
| 260 | Reduced Occupancy of the Oxygen-Evolving Complex of Photosystem II Detected in Cryo-Electron Microscopy Maps. Biochemistry, 2018, 57, 5925-5929. | 2.5 | 3 |
| 261 | Vibronic Dynamics of Photodissociating ICN from Simulations of Ultrafast Xâ€Ray Absorption Spectroscopy. Angewandte Chemie, 2020, 132, 20219-20223. | 2.0 | 3 |
| 262 | Allosteric Control of Enzyme Activity: From Ancient Origins to Recent Gene-Editing Technologies. Biochemistry, 2020, 59, 1711-1712. | 2.5 | 3 |
| 263 | Is the Supporting Information the Venue for Reproducibility and Transparency?. Journal of Physical Chemistry B, 2017, 121, 11425-11426. | 2.6 | 2 |
| 264 | Mechanistic study of CO/CO 2 conversion catalyzed by a biomimetic Ni(II)â€iminothiolate complex. International Journal of Quantum Chemistry, 2018, 118, e25555. | 2.0 | 2 |
| 265 | Nanosecond Dynamics Regulate the MIFâ€Induced Activity of CD74. Angewandte Chemie, 2018, 130, 7234-7237. | 2.0 | 2 |
| 266 | The <i>JPC</i> Periodic Table. Journal of Physical Chemistry A, 2019, 123, 5837-5848. | 2.5 | 2 |
| 267 | The <i>JPC</i> Periodic Table. Journal of Physical Chemistry Letters, 2019, 10, 4051-4062. | 4.6 | 2 |
| 268 | Computational Studies of the Oxygen-Evolving Complex of Photosystem II and Biomimetic Oxomanganese Complexes for Renewable Energy Applications. ACS Symposium Series, 2013, , 203-215. | 0.5 | 1 |
| 269 | Is the Supporting Information the Venue for Reproducibility and Transparency?. Journal of Physical Chemistry A, 2017, 121, 9680-9681. | 2.5 | 1 |
| 270 | Is the Supporting Information the Venue for Reproducibility and Transparency?. Journal of Physical Chemistry C, 2017, 121, 28212-28213. | 3.1 | 1 |

| # | Article | IF | CITATIONS |
|-----|---|------------------|--------------------------|
| 271 | The <i>JPC</i> Periodic Table. Journal of Physical Chemistry B, 2019, 123, 5973-5984. | 2.6 | 1 |
| 272 | The <i>JPC</i> Periodic Table. Journal of Physical Chemistry C, 2019, 123, 17063-17074. | 3.1 | 1 |
| 273 | Distorted Copper(II) Complex with Unusually Short CF···Cu Distances. Inorganic Chemistry, 2021, 60, 14759-14764. | 4.0 | 1 |
| 274 | Glycerol binding at the narrow channel of photosystem II stabilizes the low-spin S2 state of the oxygen-evolving complex. Photosynthesis Research, 2022, , 1. | 2.9 | 1 |
| 275 | Innenrücktitelbild: Ultrafast Solvent-Assisted Electronic Level Crossing in 1-Naphthol (Angew. Chem.) Tj ETQq1 | 1 0 78431 2.0 | 4 ₀ rgBT /Ove |
| 276 | Introducing special issue on photocatalysis and photoelectrochemistry. Journal of Chemical Physics, 2021, 154, 190401. | 3.0 | 0 |